1 **Introduction: Geology of Fractured Reservoirs**

2

3 P.A. Gillespie[1], R.E. Holdsworth[2], D. Long[3], A. Williams[1] and J.C. Gutmanis[4]

4

5 [1] Equinor ASA, Forusbeen 50, 4035, Stavanger, Norway

6 [2] Department of Earth Sciences, Durham University, Durham DH1 3LE, UK

7 [3] 2 Bucklerburn Drive, Peterculter, Aberdeen AB140XJ, UK

8 [4] Independent (JG Geology), 4 Capella Court, 42 Woodlane, Falmouth, Cornwall TR114QZ,
9 UK

10

11

12

13
14

15 **Abstract**

16 The characterisation of fractured reservoirs and fractured
17 geothermal resources requires a thorough understanding of
18 the geological processes that are involved during fracturing
19 and the host rock rheological properties. The presence or
20 absence of mechanical layering within the rock and the mode
21 of failure substantially control the organization and scaling of
22 the fracture system; subsequent chemical alteration and
23 mineralization can both increase or decrease porosity and
24 permeability. An integration of this understanding using
25 information from outcrop analogues, together with static and
26 dynamic subsurface data,can improve our ability to predict the
27 behaviour of fractured reservoirs across a range of scales.

28

29 **Keywords**

30 Fractured reservoir, geothermal, mechanical stratigraphy, basement,
31 carbonate

32

33

34 The exploration for and production of fractured reservoirs is a complex task that can prove
35 very demanding for the geoscientist. The data available are derived largely from scattered
36 wells that provide a far from complete picture of the fracture system that controls flow. A
37 critical aspect of characterising fractured reservoirs is to understand the geological setting
38 and evolution of the fracture system and the lithology of the matrix. Matrix lithology
39 determines both the brittleness of the rocks and their susceptibility to chemical alteration,
40 while the burial history underpins the diagenesis and pore-fluid history of the reservoir.
41 Fracture diagenesis may affect the growth and development of fracture systems. The stress
42 history, including tectonic events, determines the nature and development of the fracture
43 system, whilst past geological processes during fracture filling (e.g. mineralization, fault rock
44 development, sediment ingress) and present-day stress can significantly affect fracture
45 permeability.

46 The publications in this volume describe how geological understanding is used in the
47 characterisation of fractured hydrocarbon reservoirs and geothermal resources.

48 The term fracture is used generically here to mean any planar or curviplanar structural
49 discontinuity. The term "naturally fractured reservoir" refers to reservoirs that have
50 permeability and connectivity that is enhanced by the development of open natural
51 fractures. Reservoirs that contain only tight fractures, such as most porous sandstone
52 reservoirs, are not termed fractured, even if they are heavily faulted; similarly, reservoirs
53 that can only be produced following stimulation by hydraulic fracturing are not considered
54 as "naturally" fractured reservoirs.
55
56 A typical feature of fractured reservoirs is that the permeability calculated from well tests is
57 significantly higher than the permeability measured from core plugs. This is because the
58 core plug measurements record the permeability of the matrix, whereas the well tests
59 measure the effective permeability which is essentially the sum of the matrix and fracture
60 permeability. Fractures in the porous matrix enable the transfer of fluids from the matrix
61 blocks into the fracture due to the large contact surface area of the fracture. This process is
62 particularly effective where there is a large contrast between a relatively low-permeability
63 matrix and high permeability fracture, such as in many North Sea chalk reservoirs.
64 Understanding the scale of the dynamic connectivity is key for calibration of fracture
65 permeability at single well-bore to multi-well and reservoir scale.
66
67 The porosity due to fractures is usually small (usually significantly less than 1% of the rock
68 volume), but the effect of fractures on permeability can be huge. A 100 m thick porous layer
69 with 10 mD permeability has the same flow capacity as a 0.2 mm wide open horizontal
70 fracture in an impermeable layer (calculated from the Poiseuille equation for parallel plates,
71 van Golf Racht 1982). Many highly impermeable lithologies, such as cemented sandstone or
72 carbonate mudstone, are brittle and so tend to be strongly fractured. The presence of open
73 fractures allows fluids to be produced from such otherwise tight reservoirs. The flow
74 characteristics of reservoir fluids, be it oil, gas or water, can each be affected differently by
75 the rock properties of the matrix and the fractures, including wettability, relative
76 permeability and capillary pressure.

77

Types of Fractured Reservoirs

79

80 Fractured reservoirs are typically classified according to the relative contribution of
81 fractures and matrix to the reservoir porosity and permeability, such as the modified version
82 of Nelson's (2001) classification below:

83 **Type I:** fractures provide the essential reservoir porosity (ϕ) and permeability (k)

84 **Type II**: fractures provide the essential k, matrix provides storage capacity (ϕ)

85 **Type III**: fractures assist k in an already producible reservoir

86 **Type IV**: fractures provide no additional ϕ or k, but create significant reservoir anisotropy
87 (barriers)

88 This classification gives a first order indication of the production characteristics of the
89 reservoir. Type I reservoirs are typically found in basement rocks and tight carbonates. In
90 Type II reservoirs, hydrocarbons drain from the matrix blocks and into the permeable
91 fracture system, from where they are produced. Type III reservoirs have adequate matrix
92 permeability for production of fluids, in addition to permeable fractures. Type IV represents
93 reservoirs in which the fractures are less permeable than matrix (i.e. they act as baffles or
94 barriers) and are therefore not strictly fractured reservoirs in the sense used in the
95 hydrocarbon industry.
96

97 In fractured reservoirs with low matrix porosity and permeability (Type I or II above), the
98 recovery factor is sensitive to aquifer drive strength and optimization of flow rate: such
99 reservoirs are easily damaged by excessive production rates. In fractured microporous
100 reservoirs, such as chalk (Type II above), the recovery is affected by inherent rock and fluid
101 properties such as matrix permeability, fluid viscosity, wettability and fracture density (Allan
102 and Sun 2003).
103

104 Fractured hydrocarbon reservoirs can occur in a wide range of rock types, including
105 carbonates, silicified rocks, tight sandstone (e.g. tight gas sands), volcanic rocks and
106 crystalline basement (e.g. gneiss, granite). In a global database of 314 fractured oil and gas
107 reservoirs (C&C Reservoirs, 2020), carbonate reservoirs comprised 72% of the sample,
108 whereas basement reservoirs represented 8% of fractured reservoirs and volcanic reservoirs
109 only 2% (Figure 1).
110

111 The tectonic settings that have produced fractured reservoirs are variable, but out of the
112 same dataset, 50% of fractured reservoirs occur in traps that were developed during
113 contractional deformation (in the foreland or fold-thrust belt). This is in part due to the large
114 number of fractured carbonate fields that are located in the Zagros fold belt and the Rocky
115 Mountains and their forelands.
116

117 *Carbonates*

118

119 Carbonate reservoirs are highly variable, ranging from reservoirs in which the matrix
120 provides little contribution to the storage of fluids (Type I) and those with such good matrix
121 properties that fractures have little impact on overall permeability (Type III). The
122 development of fractures in carbonates is related to the depositional facies and pore types
123 that are present, as well as to the tectonic history. Carbonates are highly active chemically,
124 which means that they are prone to rapid cementation and dissolution.

125

126 Many of the largest and most productive of the world's hydrocarbon reservoirs are
127 fractured carbonate reservoirs, including the giant carbonate reservoirs of the Middle East
128 (Daniel 1954). The more recently discovered Cretaceous lacustrine reservoirs offshore Brazil
129 (commonly termed "Pre-Salt) are also influenced by fractures (e.g. Salomão et al. 2015) and
130 have become a focus of exploration and production activity since 2006.

131

132 In this thematic collection of papers, the Shaikan field of Iraq is described, which is a Jurassic
133 fractured carbonate reservoir (Gilchrist et al. **this volume**; Price et al. **this volume**) and the
134 Halalatang oilfield of the Tarim basin, China which is of Ordovician age (Ukar et al. **this**
135 **volume**).

136

137 *Crystalline basement*

138

139 Most fractured basement plays are associated with the development of up-faulted buried
140 hill traps (Biddle & Wielchowsky 1994), usually in extensional tectonic settings: the
141 reservoirs occur in the footwalls of major normal faults. Fractured granitic basement has
142 proven to be highly productive in Vietnam (Cuong and Warren 2009, Nguyen et al. 2011)
143 and in the Gulf of Suez (Salah and Alsharhan 1998, Younes et al. 1998). In both cases the
144 granitic basement has suffered deep weathering, providing additional solution-enhanced
145 porosity (P'an 1982). Commercially successful fractured basement fields are typified by long
146 hydrocarbon columns, which helps to diminish the risk of water breakthrough. They are
147 usually classified as Type I reservoirs, as the matrix permeability of crystalline basement
148 rocks is normally very low.

149

150 Recent hydrocarbon discoveries in fractured basement of the UK and the Norwegian
151 continental shelves have generated new interest in this play type. On the Norwegian
152 continental shelf, the Rolvsnes horizontal appraisal well on the Utsira High proved oil in
153 fractured and weathered granitic basement with flow rates of 7000 bopd (Trice et al. 2019).
154 In the UK, a series of discoveries have been made in the Rona Ridge, West of Shetland,
155 including the Lancaster field (Trice et al. 2019, Holdsworth et al **this volume**). The host rock
156 for the discoveries of the Rona Ridge is a Neoarchaean charnokitic basement, which is cut by
157 deep fissures extending downwards from a regional unconformity that are filled with fluids,
158 sediment and minerals (Holdsworth et al **this volume)**. The Lewisian complex in NW
159 Scotland provides a good onshore analogue for the basement rocks of the Rona Ridge, and
160 has been used to develop a conceptual understanding of the fracture system and to collect
161 quantitative fracture data that cannot be acquired from the subsurface (McCaffrey et al. **this**
162 **volume**).

163

164 *Volcanics*

165

166 Whilst hydrocarbon fields in volcanics are typically relatively small (e.g. Magara 2003), the
167 discovery of the Qingshen gas field in northeastern China, which has over 100 billion cubic
168 metres (3.5 trillion cubic feet) of gas reserves (Feng 2008), has shown that they can be large.
169 This reservoir, hosted in Cretaceous rhyolite and tuff lithologies, developed in a rift setting.
170 Gas yields are highest on palaeomorphological highs where both fractures and secondary
171 porosity are well developed, forming buried hill traps.
172
173 *Geothermal resources*

174 The production of geothermal energy requires high geothermal gradients and conductive
175 heat flux. These systems are usually associated with younger volcanics, occurring for
176 example at plate boundaries, where magma conduits exist, or in zones of high hydrothermal
177 activity (Barbier 1997) For example, the Southern Negros Geothermal field in west central
178 Phillipines, (Primaleaon et al. **this volume**) is associated with the Cuernos de Negros volcanic
179 complex; similarly, the Taupo Volcanic Zone of New Zealand contains geothermal resources
180 in volcanic rocks, crystalline plutonic rocks and metamorphosed greywacke (McNamara et
181 al. 2017). The Geysers geothermal resource in California is hosted in fractured greywacke
182 that is heated by an underlying felsite intrusion associated with the Pliocene-Holocene Clear
183 Lake volcanic field (Sammis et al 1992; Darymple et al. 1999). The permeability of many
184 geothermal systems, especially those in tight formations, depends on fracture permeability
185 with little contribution from the matrix and as such, they are directly comparable to Type I
186 fractured reservoirs. The thermal energy that is stored in the rock matrix is extracted by
187 circulation of water through the fracture system.

188 Enhanced geothermal systems (EGS or "hot dry rock" geothermal energy) produce energy
189 from deep crystalline rocks, by actively injecting water into wells to be heated and pumped
190 back out. The water is injected under high pressure which expands existing rock fractures
191 and enables the water to freely flow in and out. The lithology of EGS reservoirs is typically
192 igneous; 80% of EGS reservoirs occur in granitic rocks (data from Lu 2018). The Soultz-sous-
193 Forêts EGS project in France (Vidal and Genter 2018) is hosted in granitic rocks and overlying
194 Triassic sedimentary rocks. Here it has been found that the natural fracture permeability is
195 highest in fracture networks formed at the sediment-fracture interfaces, where a high
196 degree of geothermal alteration has occurred (Schill et al. 2017). The United Downs
197 Geothermal Power Project currently in development in Cornwall uses two wells drilled into
198 a fault zone at a depth of 2.3 to 5.2 km in high heat flow early Permian granite (Cotton et al.
199 2020). In this case, water will be injected into a natural groundwater circulation system
200 where temperatures are known to exceed 170°C.

201 **Characterisation of fractures**

202 A brief review is given below of the geological factors that control the occurrence and
203 properties of natural fractures in reservoirs. While it is difficult to make generalisations
204 without sacrificing accuracy, the aim here is to provide some broadguidance that can be
205 applied to the exploration, modelling, appraisal and development of fractured reservoirs
206 and geothermal resources.

207 *Organisation of fracturing*

208   Fractures can be classified kinematically, based on their mode of failure:

209 • **Opening mode fractures** (**joints**) are formed in conditions of tensile effective stress. They
210   are typically bedding perpendicular, forming during uplift, near surface extension or
211   folding. Opening mode fractures form perpendicular to the least compressive stress, σ_3.
212   In the subsurface, opening mode fractures may be open or may be partially to wholly
213   mineral- or sediment-filled.
214 • **Shear mode fractures** (**faults and shear fractures**), which offset markers, are formed
215   under elevated differential stress during tectonic events. Shear-mode fractures form
216   conjugate arrays that intersect parallel to σ_2 and have an acute bisector parallel to σ_1
217   (Anderson 1905, but see also Healy et al. 2015). Shear mode fractures display very
218   variable hydraulic properties.
219 • **Closing mode fractures (stylolites and compaction bands)** are formed under compressive
220   effective stress and low differential stress, perpendicular to σ_1. They are commonly
221   formed during burial but may also be tectonically driven. Closing mode fractures are
222   typically tighter than the surrounding matrix. However, if they are mechanically or
223   chemically reactivated, they can become hydraulically conductive (Graham Wall et al.
224   2006). Stylolites are typically formed during compaction of carbonates by localised
225   pressure solution and have a characteristic wavy or saw-tooth appearance. Compaction
226   bands are rarer and form only in high permeability grainy rocks, typically by a
227   combination of porosity collapse, cataclasis and pressure solution (Fossen et al. 2011;
228   Wennberg et al. 2013).

229   Under certain conditions, **hybrid fractures** may occur in which more than one mode of
230   failure is operative. For instance, in near surface conditions normal faults may develop an
231   opening mode component (Holdsworth et al. **this volume**).

232   The fracture classification described above is fundamental, and the different classes of
233   fractures have differing geometry and scaling properties. However, it is not always
234   straightforward to distinguish the kinematic origin of fractures from subsurface data, so a
235   more pragmatic approach may be needed when describing the fractures from wells. In
236   particular, it is difficult to distinguish between small shear-mode fractures with no clearly
237   visible displacement and opening mode fractures. In practice, fractures in wells may be
238   categorised as "**faults**" which have clear shear offset (or supporting evidence from
239   biostratigraphy) and "**fractures**" which have no clear shear offset; the latter category may in
240   reality include both opening mode and shear mode fractures. In many natural fracture
241   systems, shear and opening mode fractures are closely interlinked (Kim et al. 2003) and
242   understanding their kinematic relationship may difficult from subsurface data. Closing mode
243   fractures such as stylolites can usually be identified from borehole image or core data. Any
244   fracture classification based on image logs should be calibrated against core data, where
245   available, in order to determine the fracture kinematics and fill.
246
247   The vertical extent of fractures exerts an important control on vertical effective permeability
248   and capillary continuity. The vertical propagation of natural fractures is controlled by
249   mechanical contrasts and by the stress in the mechanical units. Fractures which are
250   contained within individual mechanical units are termed *stratabound*, while fractures that
251   extend through many units are termed *non-stratabound* (Figures 2 - 4; Odling et al. 1999).

252 Non-stratabound joints tend to form in clusters (Gillespie et al. 1999; Gillespie et al. 2001)
253 and clusters of sub-parallel joints are sometimes termed fracture corridors (De Keizer et al.
254 2007; Questiaux and Couples 2010; Laubach et al. 2018).
255
256 Stratabound joints tend to be regularly spaced and form a continuous organised network. In
257 modelling, this kind of fracturing is referred to as background fracturing. Where jointing
258 units are separated by non-jointing units (Figure 4), the stratabound joints typically have a
259 spacing that is proportional to the thickness of the jointing unit (Huang and Angelier 1989;
260 Narr and Suppe 1991; Gross et al. 1995), or alternatively the fractures may develop in a
261 series of regularly spaced clusters (Gillespie et al. 1999; Philip et al. 2005) However, many
262 sedimentary fractured reservoirs consist of a stack of jointing units that are not separated
263 by non-jointing units. In this case the mechanical unit thickness is not well-defined and a
264 hierarchy of joints may occur at different scales (Strijker et al. 2012; Laubach et al. 2018;
265 Corradetti et al. 2018; Gutmanis et al. 2018).
266
267 The simple relationship described above, in which the spatial organization of the fractures is
268 controlled by their vertical extent through the stratigraphy, is not the complete picture, as
269 the degree of fracture cementation also plays a role. Detailed field and subsurface
270 observations indicate that fractures that are uncemented tend to be regularly or randomly
271 spaced, whereas fractures that are partially cemented are more likely to be clustered
272 (Hooker et al. 2013; Li et al. 2019).
273
274 In order to quantify the fracturing in stratified rocks, the *fracture stratigraphy* should be
275 described, i.e. the variation in fracture extent and occurrence within the different units
276 (Corbett et al. 1987; Bertotti et al. 2007; Laubach et al. 2009; Morris et al. 2009; Zahm and
277 Hennings 2009). The term fracture stratigraphy is sometimes conflated with *mechanical*
278 *stratigraphy*, which describes the mechanical changes in rocks in relation to the stratigraphy
279 (Laubach et al. 2009). Understanding the fracture stratigraphy and the mechanical
280 stratigraphy and how they evolved is important for the correct placement and completion of
281 wells and helps in the definition of flow units within the reservoir. Ductile layers or weak
282 interfaces represent mechanical contrasts which tend to impede the vertical propagation of
283 fractures. This mechanism is important in limiting vertical effective permeability in layered
284 heterogeneous rocks. In stacked units of similar elastic properties, the principle parameters
285 controlling vertical joint propagation are the frictional properties of the interface and the
286 depth at time of deformation and since the friction is greater on deeper interfaces, non-
287 stratabound fractures are more prone to occur at significant depth (Gillespie et al. 2001).

288 Mechanical contrasts can be seen in igneous intrusions of different types. Felsic igneous
289 plutons are typically unstratified, and so clustered, or irregular non-stratabound joints
290 develop (Segall and Pollard 1983; Bertrand et al. 2015). However, in layered igneous
291 intrusions or in metamorphic rocks, stratification may influence the fracturing (e.g. Foster
292 and Hudleston 1986). In volcanic sills and lava flows, polygonal jointing may occur due to
293 stress built up during cooling, providing a very well-connected fracture network (Hetényi et
294 al. 2012; Gudmundsson & Løtveit 2012; Walker et al. 2013). In the oil-producing sills of the
295 Nequen Basin, Argentina, the open fractures are thought to be a combination of cooling
296 joints and tectonically induced fractures (Witte et al. 2012).

297   Tectonic faults tend to be non-stratabound, unless they reach a ductile layer such as a
298   mobile shale or an evaporite unit (Ferrill et al. 2014). Tectonic faults are clustered (Gillespie
299   et al. 1993, Johri et al. 2014), and are often surrounded by diffuse zones of fracturing
300   termed *damage zones* (Figure 5; Solum & Huisman 2017; Gutmanis et al. 2018, McCaffrey et
301   al. **this volume** Figure 3f). Damage accumulates at asperities along the fault and at branch
302   lines, relay zones and fault intersections (Rotevatn and Bastesen 2014; Nixon et al. 2019).
303   Damage zones associated with faults that are large enough to cut through the entire
304   reservoir can provide high permeability pathways that dominate fluid flow both vertically
305   and horizontally (Paul et al. 2009).

306   ### *Conditions of fracture formation*

307   According to the principles of rock mechanics, opening mode and shear fractures develop
308   under distinct stress conditions. Faults are formed under elevated differential stress,
309   typically during tectonic events. Joints form under conditions of low differential stress (Price
310   and Cosgrove 1990) and are therefore less likely to form during tectonic events, in which
311   differential stress is high. Joint formation requires the effective stress be tensile, which can
312   happen close to the surface or at elevated pore fluid pressure; joints can form during uplift
313   as a result of thermal and elastic contraction (Engelder 1993). Care must be taken in using
314   outcrop analogues of joint systems, as not all of the fracture sets observed at the surface
315   may be present in the subsurface.

316   Gravitational collapse of caverns can cause extensive brecciation (Daniels et al. 2020), as can
317   events of overpressure related to faulting (Sibson 1996) or volcanic processes. In breccias,
318   the fractures may have components of both opening and shear mode.

319   In the subsurface it is important to analyse the wider, potentially basin-scale, depositional
320   and tectonic history in order to reconstruct the framework of faulting and fracturing
321   styles.Geologically heterogeneous sequences can lead to a large degree of local stress
322   variation, resulting in many different fault and fracture types and fracture-intersection
323   relationships, which can often only be deciphered at outcrop.

324   ### *Joint aperture and fill*
325
326   Opening-mode fractures create voids and the size of these voids are altered by chemical
327   processes, namely precipitation and dissolution (Wennberg et al. 2016; Lima and De Ros
328   2019). In a chemically inactive system, such as may occur at shallow depths, joints have a
329   mechanical aperture (opening) that is controlled by mechanical parameters alone. Under
330   conditions of elevated pore fluid pressure, joints may be fully open, with an aperture
331   controlled by the effective stress and the rock properties. At lower fluid pressures the walls
332   of the fracture are partially in contact and the fracture aperture is defined by patches of the
333   fracture that are not in contact, which reduce in area as the effective compressive stress
334   increases (Pyrak-Nolte et al. 2000). In more chemically active systems, the aperture of the
335   joint may become occluded by precipitating minerals (Laubach et al. 2004; Gale et al. 2010;
336   Wennberg et al. 2016; Laubach et al. 2019), leading to a decrease in reservoir productivity
337   (Laubach 2003). These are variously referred to as cemented, healed or sealed fractures
338   (Anders et al. 2014 for review of the terminology).
339

340   *Fault properties*
341
342   Faults have highly variable lithological and mineralogical content, according to the
343   mechanical properties of the host rock together with the fluid and stress history (see Bense
344   et al. 2013 for review). In porous sandstone or grainstone, deformation within the damage
345   zone is accommodated by compactional shear, leading to the formation of deformation
346   bands (more precisely, shear bands), that have lower permeability than the host rock
347   (Micarelli et al. 2006; Wennberg et al. 2013; Kaminskaite et al. 2019). More commonly, in
348   rocks of low porosity (e.g. carbonate mudstone or crystalline basement), faults are
349   accommodated by dilational shear, in which open fractures and an open fault breccia is
350   developed, so that faults become hydraulically conductive (Crawford and Yale 2002).
351   Experience from fractured reservoirs indicates that faults tend to be highly conductive, but
352   they can also act as combined barriers and conduits (e.g. Caine et al. 1996; Agosta 2008).
353
354   The porosity in the fault zone may be occluded by precipitation of minerals (Woodcock et al
355   2007). Fault reactivation tends to cause breakage of mineral fills and re-opening of the fault;
356   the faults that have most recently been active are those that are most likely to be open. In
357   cases where open fractures are only partially filled, the fill can act as a natural prop
358   counteracting the effects of in-situ stress loading and enhancing long-term permeability of a
359   fractured reservoir (Holdsworth et al. 2019). Where there is shale in the faulted sequence,
360   the shale may be smeared into the fault zone and form a baffle to fluid flow (Færseth 2006;
361   Bastesen et al. 2010); fault-gouge and clay smear can significantly diminish the conductive
362   properties of the fault, both across and along the fault plane.
363

364   *Fracture size*

365   The fracture size is defined by its vertical extent (height), lateral extent (length) and
366   aperture (opening).

367   The length distribution of fractures is one of the principal controls on the connectivity and
368   permeability of the fracture system (de Dreuzy et al. 2001; Philip et al. 2005). In the
369   subsurface, the horizontal extent, or fracture length, cannot be readily measured below
370   seismic scale, requiring the use of outcrop analogues for their elucidation. Alternatively, the
371   size distribution of faults imaged using seismic reflection data can be extrapolated
372   downscale using an assumed size distribution (Yielding 1996).

373   In the case-of non-stratabound fractures, there is no characteristic length scale that controls
374   the size of the fractures, so their horizontal extent and maximum displacement tend to
375   follow a power-law (Pareto) cumulative frequency distribution typical of fractals (Odling et
376   al. 1999; Gillespie et al. 2001; Bertrand et al. 2015). In stratabound examples, the
377   mechanical unit thickness typically imparts a characteristic spacing to the fractures (Bai and
378   Pollard 2000; Schöpfer et al. 2011) and their length is controlled by interaction with other
379   joints (Gross et al. 1993). This means that stratabound fractures tend not to follow non-
380   power law size distributions and are not fractal (Gillespie et al. 1999). As stratabound
381   fracture systems tend to divide the rock matrix into a series of blocks of regular size, the
382   effective permeability of the fractured rock can be assigned a representative elementary

383 volume (Bear 1972; Odling et al. 1999; Müller et al. 2010). However, in fracture systems that
384 have power law size distribution and clustered spatial distribution, the definition of
385 representative elementary volume may not be possible.

386

387 The aperture of subsurface fractures is difficult to estimate directly and surface apertures
388 may be unrepresentative of subsurface fractures due to thechanging stress conditions
389 occurring at different depths. However, partially cemented fractures have an aperture at
390 the surface that is less sensitive to stress and so study of veins and partially cemented
391 fractures can provide useful information (Laubach et al. 2016; Laubach 2019). In this
392 context, it is important to distinguish between the distance between the fracture walls, or
393 kinematic aperture and the true aperture which is the distance across the void within the
394 fracture.

395 In a study of veins (fully cemented fractures) from a range of sedimentary rocks, Gillespie et
396 al. (1999) concluded that veins typically have kinematic apertures that follow power law
397 cumulative frequency distributions in non stratabound fracture systems, but they are non-
398 power law in stratabound fracture systems. However, Ortega et al. (2006) reported
399 stratabound fractures veins in carbonate host rocks and found them to have a power law
400 kinematic aperture distribution. Additionally, Hooker et al. (2013, 2014) have demonstrated
401 from detailed examination of fractures in sandstone that the process of fracture
402 cementation can have a fundamental effect on the size distributions of fractures: power-law
403 kinematic aperture size distributions are favoured in cases where fracture growth is
404 unevenly distributed amongst variably cemented fractures.

405

406 In Type I fractured reservoirs, the fracture porosity dominates the storage potential of the
407 reservoir and so accurate determination of the fracture size, including the fracture height,
408 length and aperture, is critical for commercial development.

409 Comprehensive analyses of multi-scale size distributions of fractures are given from the
410 Lewisian Complex by McCaffrey et al. (**this volume**), and from volcanics by Primaleon et al.
411 (**this volume**). In both areas, composite cumulative frequency plots of fracture length show
412 approximately power law distributions of several orders of magnitude, although in the
413 poorly exposed volcanics (Primaleon et al. **this volume**), there is a marked change in
414 exponent between regional scale datasets from maps and smaller scale data derived from
415 outcrop and core. In each of these studies, the scaling of the fracture kinematic aperture
416 (the distance between the fracture walls, regardless of fill) was also analysed. In both
417 datasets, the kinematic aperture shows a broadly power-law cumulative frequency
418 distribution, with higher observed frequencies of small aperture fractures in core data than
419 in outcrop data. In the Lewisian rocks of the Lancaster discovery, subsurface aperture
420 measurements derived from electrical logs also fall broadly onto a power-law cumulative
421 frequency distribution when different samples are plotted onto a single graph, although
422 individual samples do not conform to power-law size distributions. (Holdsworth et al. **this
423 volume**).

Joint density and lithology

Opening-mode fractures (joints) cannot develop in cohesionless materials, and consideration of the Griffith/Navier-Coulomb failure criterion shows that rock with low cohesion, such as poorly cemented sand or porous carbonate grainstone, opening mode fractures can only develop under conditions of very low differential stress (e.g. Price and Cosgrove 1990). Hence opening mode fractures are rare or absent in high porosity reservoir sandstone or limestone unless they have been subjected to elevated pore-pressure. However, as cementation increases, porosity and pore throat sizes decrease and cohesion increases, making the rock become more brittle and prone to fracture. Thus, by pure serendipity, as the matrix loses permeability by cementation, the reservoir is more likely to have a component of fracture permeability. An example of this effect is seen in the Valhall chalk field, where fractured hardgrounds provide high permeability zones within the reservoir (Tjetland et al. 2007).

Surface and subsurface observations indicate that the density of joints varies strongly according to the brittleness of the rock at the time of deformation. As a rough guide, the relative brittleness of different rock types can be expressed as: silica > tight carbonate > porous carbonate > clay or organic-rich shale. Similarly, quartz-cemented sandstone is more prone to fracturing than porous sandstone. The presence of clay minerals can weaken the rock and make it significantly less brittle, so clay-rich carbonates tend to have lower fracture density than clean carbonates (Laubach et al. 2009).

Fracture connectivity

The connectivity of the fracture system is one of the most important controls on the effective permeability of fractured networks and has been investigated using percolation theory (Long and Witherspoon 1990). At low fracture density, fractures tend to be disconnected and so have limited contribution to effective permeability (but see also Philip et al. 2005 and Olson et al. 2009). At high density, the fractures are fully connected leading to a fracture system that is highly permeable. At intermediate density, fractures start to become connected and may form a number of isolated connected networks. The point at which the fracture system becomes connected across the reservoir is called the percolation threshold and is controlled by the total fracture density, the fracture size, and their orientation distribution (Hestir and Long 1990).

The number and type of fracture intersections are important factors in which influence fracture network connectivity. Measurements of fracture topology from core or from surface data allow rigorous quantification connectivity (Manzocchi 2002; Sanderson and Nixon 2015; Sanderson and Nixon 2018). Using these techniques, McCaffrey et al. (**this volume**) and Holdsworth et al. (**this volume**) showed high degree of connectivity of fractures in Lewisian basement at outcrop and at in the basement of the Rona Ridge. In a multiscale study of the volcanic rocks of the Southern Negros geothermal field, Primaleon et al. (**this volume)** found high fracture connectivity and were able to establish that connectivity is greater close to large faults. Unfortunately, the connectivity of the fracture

468   system to an individual well cannot be uniquely determined from static subsurface data
469   alone, as the details of the fracture topology cannot be mapped far from the borehole.
470   However, we can infer connectivity from pressure data, interference tests and the use of
471   tracers (see Narr et al. 2006 and Price et al. **this volume** for examples).

472
473   *Factors causing fracture localization*

474
475   An important aspect of fractured reservoir characterisation is the understanding of the
476   factors that cause localization and change in orientation of fractures. Regions that are highly
477   fractured often represent high-permeability zones, which could act as areas of high well
478   productivity, or areas of early breakthrough of injected water or gas. In the former case it
479   pays to target highly fractured regions, whereas in the latter they should be avoided; getting
480   this right or wrong can determine the commercial success or failure of a field.

481
482   The damage zone model of fault-related fracturing is widely used in reservoir modelling (e.g.
483   Gauthier et al. 2002) and implies localized high permeability zones of open fractures
484   associated with faults. However, stratabound joints that form when the faults are active
485   may be more homogeneously distributed, with their orientation determined by local stress
486   perturbations around the faults (e.g. Rawnsley et al. 1992; Bourne et al. 2001).

487
488   Clusters of opening mode fractures, or fracture corridors, may be due to local stress
489   concentrations, such as may occur close to faults. However, in many cases there are no
490   obvious causes of stress heterogeneity. Olson (2004) has shown using mechanical modelling
491   that clusters of joints may occur spontaneously in a growing set of fractures due to the
492   interaction of the stress fields around each fracture. Hence prediction of fracture corridors is
493   challenging and there is a reliance instead on direct detection using well data or seismic
494   techiques (Ozkaya 2007; Nosjean et al. 2020).

495
496   Folding can cause localization of fracturing. For example, in the thrust-related folds of the
497   Canadian foothills, successful gas wells are targeted into the hinges or forelimbs of folds
498   (Cooper et al. 2004). However, not all the fractures in a fold are related to the folding event;
499   some may have developed before and others after the event, in which case their fracture
500   density and orientation may not be related to fold geometry (Ahmadhadi et al. 2008;
501   Shackleton et al. 2011; Casini et al. 2011; Tavani et al. 2018).

502
503   Various techniques can be used to predict fracture density and orientation. In a simple static
504   approach, the curvature of horizons may be used to estimate fracture density (Stewart &
505   Podolski 1998; Bergbauer & Pollard 2003). In faulted areas, the distance from faults may be
506   used to condition the density of fractures. Otherwise, geomechancial modelling can used to
507   estimate the stress/strain at the time of deformation, and thereby to estimate fracture
508   parameters (Bourne et al. 2001; Maerten et al. 2019). Regardless of the technique that is
509   used, results must be carefully calibrated against seismic and well data and supported by
510   outcrop analogue data where appropriate.

511
512   *In situ stress*

513

514 The orientation and magnitudes of *in-situ* stress can have a significant impact on fracture
515 aperture, and hence the effective permeability tensor of fractured formations. As the
516 reservoir fluid pressure is depleted, the effective stress changes and fractures may close,
517 becoming less permeable: such reservoirs are called "stress-sensitive". However, rough
518 walled or partially filled cemented fractures may become locked open, or propped, making
519 the reservoirs less sensitive to stress (Dyke and Hudson 1992).
520
521 Wellbore temperature monitoring in fractured crystalline basement has shown that the
522 fractures most likely to be open and permeable are those that are oriented relative to stress
523 field in such a way that they are on the verge of slipping, leading to the concept of "critically
524 stressed" fractures (Barton et al. 1995). Gilchrist et al. (**this volume**) give evidence that in
525 the carbonates of the Shaikan field in Kurdistan, the fractures remain critically stressed even
526 after depletion of the reservoir; they argue that, in such seismically active regions, the
527 tectonic stress will build up again until the system reaches criticality. The continued
528 criticality of the fracture system may allow the reservoir to maintain high effective
529 permeability during depletion, but the critically stressed fractures may also present
530 problems for wellbore integrity.
531
532 ***Chemical modification of fractured systems***

533 Carbonate reservoirs often have a complex diagenetic history, with diagenetic processes
534 frequently controlled or influenced by phases of fracturing (Smith and Davies 2006; Sharp et
535 al. 2010). When carbonate rocks are exposed in a humid environment, or under certain
536 conditions in the subsurface, they may undergo dissolution to form karst (Loucks 1999,
537 White 2016), a phenomenon in which carbonate or evaporite minerals are dissolved to form
538 macroscopic vugs and caves. Karst dissolution enlarges the aperture of pre-existing fractures
539 with an increase in porosity and permeability. However, porosity may also become blocked
540 by sediment or by precipitation of diagenetic minerals. As a result, karst reservoirs are often
541 complex. They share many of the production characteristics of fractured reservoirs,
542 although the additional presence of open voids and caverns can lead to extremely
543 heterogeneous production characteristics and reservoir behaviour. Drill-bit drops and high
544 instantaneous mud-loss rates are typical experiences in highly karstified reservoirs (Mazullo
545 and Chilingarian 1996; Loucks 1999).
546
547 Under some conditions, dissolution of carbonates can occur in the deep subsurface
548 (Mazzulo and Harris 1992), although there is controversy around whether this process can
549 generate significant porosity (Ehrenberg et al. 2012). Nevertheless, there is evidence that
550 late-stage dissolution and vug formation can occur at depth in association with fractures.
551 Ukar et al. (**this volume**) argue that in the Halahatang oilfield of the Tarim Basin, which is
552 hosted by Ordovician carbonate rocks, cavernous porosity developed at moderate depths in
553 a series of dissolution events.
554
555 Caverns developed by karst dissolution of carbonate or evaporite can collapse, causing
556 intense fracturing and brecciation of the overlying rocks (e.g. Daniels et al. 2020, Ukar et al.
557 **this volume**). These zones can be associated with enhanced production rates, as found in
558 the Ellenburger Group carbonates of Texas (Loucks 1999).
559

560 Early and pervasive cementation of the carbonate platform causes embrittlement, leading
561 to the development of major syn-depositional fracture systems behind the margin of steep-
562 sided platforms (Hunt et al. 2003, Frost and Kerans 2010, Nolting et al. 2020). This can have
563 important consequences for production, for example in the Paleozoic super-giant Tengiz
564 field in Kazakhstan (Narr and Flodin 2012), and the Devonian-aged Kharyaga field in Russia,
565 (Spina et al. 2015).
566
567 Crystalline basement is, by its nature, rock of very low porosity and permeability, which
568 depending on mineralogy commonly has low chemical reactivity. Development of fractures
569 in crystalline basement may not provide sufficient storage for commercial reservoir
570 potential, as the porosity of unaltered fractures is very low. Some degree of chemical
571 alteration may therefore be required to generate a hydrocarbon reservoir, and this may be
572 provided by chemical weathering if the basement is exposed over a very long time.
573 Therefore, productive basement reservoirs typically underlie major unconformities (P'An
574 1982; Koning 2003; Holdsworth et al. **this volume**). Fractures formed close to the
575 weathering surface may form open fissures that extend down into the underlying basement
576 and focus descending or ascending fluids, leading to fracture porosity and permeability
577 enhancement by chemical and mechanical weathering.

578 Hydrothermal alteration is commonly observed in crystalline basement rocks. In some
579 geothermal reservoirs, hydrothermal circulation allows the precipitation of geothermal
580 minerals that can prop open or occlude the fractures. In Soultz-sous-Forêts the wall rocks of
581 the fractures have been intensely transformed by hydrothermal alteration and the mineral
582 assemblage must be characterized in order to design the best stimulation (Ledésert et al.
583 2010). In the Lancaster oil field of the UK's Rona ridge, a near surface hydrothermal system
584 was associated with fractures in the basement (Holdsworth et al. this **volume**). The
585 hydrothermal minerals that were generated from this system propped open the fissures,
586 allowing storage of oil.

587 **Data acquisition**

595 The subsurface data available for the characterisation of fracture networks consists of
596 seismic data and well data. Seismic reflection data are of limited spatial resolution, and as
597 such can only image large faults. Well data are of much higher resolution, but do not
598 capture the key characteristics of any of the larger fractures. Between seismic data and well
599 data exists a range of scales at which fractures cannot be directly sampled. This is known as
600 the resolution gap, for which outcrop analogues and remote sensing can provide important
601 proxy data.
602
603 Seismic reflection data are important for mapping the larger structures such as faults,
604 although the vast majority of fractures will not be directly detectable. Seismic anisotropy
605 can also be used to infer the presence and orientation of fractures under suitable
606 conditions. Newly developed methods for extracting faults and fractures from seismic data
607 are showing promise and can be a useful adjunct to manual interpretation (e.g. Bonter and
608 Trice 2019; Wu et al. 2019).
609

610 Core provides essential information about the content of fractures and the density and
611 small-scale connectivity of the fracture network. CT scans of core can yield 3-D volume
612 renditions of the fractures in the core barrel, before the core is damaged by further handling
613 (Wennberg et al. 2009). However, the most intensely fractured reservoir intervals typically
614 result in zones of no recovery or 'rubble zones' and so are under-sampled by coring.

616 Borehole imagery allows the determination of fracture orientation and properties
617 (Poppelreiter et al. 2010), and the quality of borehole images is steadily improving. Acoustic
618 and resistivity-based tools are both valuable and yield complementary results and
619 integration with core data can provide calibration of the results (Fernández-Ibáñez et al.
620 2018). Borehole imagery is also used to determine the direction of *in situ* stress, which can
621 affect fracture permeability (e.g. Gilchrist et al. **this volume**).

623 In the absence of borehole imagery, conventional wireline logs can provide information
624 about fracturing. For instance, the caliper, sonic and photoelectric logs are all sensitive to
625 fracturing and can indicate fractured zones in the well.

627 While information about the size and connectivity of fractures is very limited from well data,
628 outcrops can provide a wealth of data about the extent of fractures, their fills and their
629 relation to lithology and geological structure. Fieldwork can be supplemented by the use of
630 remote sensing data, and also increasingly by virtual outcrop models derived from LiDAR or
631 from drone-based digital photogrammetry (e.g. Pearce et al. 2011; Gillespie et al. 2011;
632 Vollgger and Cruden 2016; Corradetti et al. 2018).

634 Dynamic data such as production tests and interference tests are essential for
635 determination of the effective permeability. Mud losses and gas kicks can also provide
636 dynamic information about the fracture system (Alvarez et al. 2015), with use of systems
637 such as real time mud gas monitoring micro mud-loss meters that are designed to optimize
638 collection of this information.

639 In an optimal workflow, the fracture network is represented as a discrete fracture network
640 (DFN) and the pressure derivative of the well test is matched by adjusting the matrix and
641 fracture parameters. In this way, the geological and engineering concept of the fractured
642 reservoir can be fully integrated. A good example of this workflow applied to the fractured
643 carbonate Shaikan field is given in Price et al. (**this volume**). DFNs were created for
644 individual well tests using all of the available geological data and adjusted to match the well
645 test pressure derivatives. The DFNs were then validated by simulation of transient bottom
646 hole pressures and pressure interference data. The field scale DFN was then upscaled to a
647 full-field dynamic simulation model for use in production forecasting.

648 **Conclusions**

649 An understanding of the geological controls on fracture system development and
650 organisation is fundamental to developing viable concepts of fracturing that can be used in
651 assessing fractured hydrocarbon and geothermal reservoirs. Host rock lithology and stress
652 conditions effect the organization and scaling of fracture systems and the development of

653 stratabound, non-stratabound or hierarchical fracture systems. The degree of chemical
654 modification depends on the primary composition of the host rock as well as on the
655 geofluids that were present. When fractures occur at the surface they may be strongly
656 altered and may be filled with sediment, altering their hydraulic properties. Use of data
657 from core and outcrop analogues is important for understanding the geological
658 development of fractures, but the addition of other data sources such as seismic, borehole
659 image data and dynamic data allows for a more complete definition of the hydraulic effect
660 of the fracture systems.

661 The papers in this volume intend to give some good examples of how a proper geological
662 understanding and quantitative analysis of fracture systems improves our ability to make
663 useful predictions in the subsurface.

664

Acknowledgements

668

References

669 **References**

671 Agosta, F. (2008). Fluid flow properties of basin-bounding normal faults in platform
672 carbonates, Fucino Basin, central Italy. *Geological Society, London, Special*
673 *Publications*, *299*(1), 277-291.

675 Ahmadhadi, F., Lacombe, O., & Daniel, J. M. (2007). Early reactivation of basement faults in
676 Central Zagros (SW Iran): evidence from pre-folding fracture populations in Asmari
677 Formation and lower Tertiary paleogeography. In Thrust Belts and Foreland Basins (pp. 205-
678 228). Springer, Berlin, Heidelberg.

680 Allan, J., & Sun, S. Q. (2003). Controls on recovery factor in fractured reservoirs: lessons
681 learned from 100 fractured fields. In SPE Annual Technical Conference and Exhibition.
682 Society of Petroleum Engineers.

684 Alvarez, S. F., Cazuriaga, G. V., Martocchia, A., & Chamon, O. (2015). Evaluation of a
685 Fractured Tight Reservoir in Real-Time: The Importance of Detecting Open Fractures while
686 Drilling with Accurate Mud Flow Measurement. *AAPG# 2102787. Denver, CO, USA*.

688 Anders, M. H., Laubach, S. E., & Scholz, C. H. (2014). Microfractures: A review. *Journal of*
689 *Structural Geology*, *69*, 377-394.

691 Anderson E.M. (1904) The dynamics of faulting. Transactions of the Edinburgh Geological
692 Society, 8, 387-402, https://doi.org/10.1144/transed.8.3.387

694 Bai, T., & Pollard, D. D. (2000). Fracture spacing in layered rocks: a new explanation based
695 on the stress transition. Journal of Structural Geology, 22(1), 43-57.

697 Barbier, E. (1997). Nature and technology of geothermal energy: a review. Renewable and
698 sustainable energy reviews, 1(1-2), 1-69.

700 Barton, C. A., Zoback, M. D., & Moos, D. (1995). Fluid flow along potentially active faults in
701 crystalline rock. Geology, 23(8), 683-686.

703 Bastesen, E., & Braathen, A. (2010). Extensional faults in fine grained carbonates–analysis of
704 fault core lithology and thickness–displacement relationships. Journal of Structural
705 Geology, 32(11), 1609-1628.

706 Bear J (1972) Dynamics of fluids in porous media. Environmental science series. Elsevier,
707 Amsterdam, p 784.

708

709 Bense, V. F., Gleeson, T., Loveless, S. E., Bour, O., & Scibek, J. (2013). Fault zone
710 hydrogeology. *Earth-Science Reviews*, *127*, 171-192.

711

712 Bergbauer, S. & Pollard, D.D. 2003. How to calculate normal curvatures of sampled
713 geological surfaces. *Journal of Structural Geology*, **25**, 277–289.
714
715
716 Bertotti, G., Hardebol, N., Taal-van Koppen, J. K., & Luthi, S. M. (2007). Toward a
717 quantitative definition of mechanical units: New techniques and results from an
718 outcropping deep-water turbidite succession (Tanqua-Karoo Basin, South Africa). *AAPG*
719 *bulletin*, *91*(8), 1085-1098.

720

721 Bertrand, L., Géraud, Y., Le Garzic, E., Place, J., Diraison, M., Walter, B.& Haffen, S. (2015). "A
722 multiscale analysis of a fracture pattern in granite: A case study of the Tamariu granite,
723 Catalunya, Spain." *Journal of Structural Geology* 78, 52-66.

724

725 Biddle, K. T. and Wielchowsky, C. C., 1994. Hydrocarbon Traps: Chapter 13: Part III. Processes.
726 In: Magoon, L. & Dow, W. (ed.) The Petroleum System - From Source To Trap. AAPG Memoir
727 60, 219-235.

728

729 Bonter, D. A., & Trice, R. (2019). An integrated approach for fractured basement
730 characterization: the Lancaster Field, a case study in the UK. *Petroleum Geoscience*, *25*(4),
731 400-414.

732

733 Bourne, S.J., Rijkels, L, Stephenson, B.J., Willemse, E.J.M. 2001. Predictive modelling of
734 naturally fractured reservoirs using geomechanics and flow simulation. GeoArabia, 6, p 27-
735 42.

736

737 C&C Reservoirs (2020), DAKS 4.0. Unpublished.

738

739   Caine, J. S., Evans, J. P., & Forster, C. B. (1996). Fault zone architecture and permeability
740   structure. *Geology*, *24*(11), 1025-1028.

741   Casini, G., Gillespie, P. A., Vergés, J., Romaire, I., Fernández, N., Casciello, E., ... & Aghajari, L.
742   (2011). Sub-seismic fractures in foreland fold and thrust belts: insight from the Lurestan
743   Province, Zagros Mountains, Iran. Petroleum Geoscience, 17(3), 263-282.

744

745   Cooper, M., C. Brealey, P. Fermor, R. Green, and M. Morrison, 2004, Structural models of
746   subsurface thrust-related folds in the foothills of British Columbia— Case studies of
747   sidetracked gas wells, in K. R. McClay, ed., Thrust tectonics and hydrocarbon systems: AAPG
748   Memoir 82, p. 579–597.

749

750   Corbett, K., Friedman, M., & Spang, J. (1987). Fracture development and mechanical
751   stratigraphy of Austin Chalk, Texas. *AAPG Bulletin*, *71*(1), 17-28.

752

753   Corradetti, A., S. Tavani, M. Parente, A. Iannace, F. Vinci, C. Pirmez, S. Torrieri, M. Giorgioni,
754   A. Pignalosa, and S. Mazzoli. (2018) "Distribution and arrest of vertical through-going joints
755   in a seismic-scale carbonate platform exposure (Sorrento peninsula, Italy): insights from
756   integrating field survey and digital outcrop model." *Journal of Structural Geology* 108, 121-
757   136.

758

759   Cotton, L., Gutmanis, J., Shail, R., Dalby, C., Batchelor, T., Foxford, A. and G. Rollinson. (2020)
760   Geological overview of the United Downs deep geothermal power project, Cornwall, UK.
761   Proceedings World Geothermal Congress, Reykjavik, Iceland, April 26 – May 2, 2020.

762

763   Crawford, B. R., & Yale, D. P. (2002). Constitutive modeling of deformation and permeability:
764   relationships between critical state and micromechanics. In *SPE/ISRM Rock Mechanics*
765   *Conference*. Society of Petroleum Engineers.

766

767   Cuong, T. X., & Warren, J. K. (2009). Bach ho field, a fractured granitic basement reservoir,
768   Cuu Long Basin, offshore SE Vietnam: A "buried-hill" play. *Journal of Petroleum*
769   *Geology*, *32*(2), 129-156.

770

771   Dalrymple, G. B., Grove, M., Lovera, O. M., Harrison, T. M., Hulen, J. B., & Lanphere, M. A.
772   (1999). Age and thermal history of the Geysers plutonic complex (felsite unit), Geysers
773   geothermal field, California: a 40Ar/39Ar and U–Pb study. *Earth and Planetary Science*
774   *Letters*, *173*(3), 285-298.

775

776 Daniel, E. J. 1954. Fractured Reservoirs of Middle East. Bulletin of the American Association
777 of Petroleum Geologists, 38(5), 774–815.

778

779 Daniels, S.E., Tucker, M.E., Mawson, M.J., Holdsworth, R.E., Long, J.J., Gluyas, J.G. and Jones,
780 R.R. 2020. Nature and origin of collapse breccias in the Zechstein of NE England: local
781 observations with cross-border petroleum exploration and production significance, across
782 the North Sea. *In:* Georgiopoulou, A., et al. (eds) *Subaqueous Mass Movements and their*
783 *Consequences: Advances in Process Understanding, Monitoring and Hazard Assessments.*
784 Geological Society, London, Special Publications, 494, https://doi.org/10.1144/SP494-2019-
785 140

786

787 de Dreuzy, J. R., Davy, P., & Bour, O. (2001). Hydraulic properties of two-dimensional
788 random fracture networks following a power law length distribution: 2. Permeability of
789 networks based on lognormal distribution of apertures. Water Resources Research, 37(8),
790 2079-2095.

791

792 De Keijzer, M., Hillgartner, H., Al Dhahab, S., & Rawnsley, K. (2007). A surface-subsurface
793 study of reservoir-scale fracture heterogeneities in Cretaceous carbonates, North
794 Oman. Geological Society, London, Special Publications, 270(1), 227-244.
795
796 Dyke, C. G. and Hudson, J.A. (1992). Stress insensitive natural fracture permeability within
797 hydrocarbon reservoirs. In *Rock Characterization: ISRM Symposium, Eurock'92, Chester, UK,*
798 *14–17 September 1992* (pp. 281-286). Thomas Telford Publishing.

799

800 Ehrenberg, S. N., Walderhaug, O., & Bjørlykke, K. (2012). Carbonate porosity creation by
801 mesogenetic dissolution: Reality or illusion? *AAPG bulletin*, *96*(2), 217-233.

802

803 Engelder, T. 1993. Stress Regimes in the Lithosphere. Princeton University Press, pp. 457.

804

805 Færseth, R. B. (2006). Shale smear along large faults: continuity of smear and the fault seal
806 capacity. Journal of the Geological Society, 163(5), 741-751.
807
808
809 Feng, Z. Q. (2008). Volcanic rocks as prolific gas reservoir: A case study from the Qingshen
810 gas field in the Songliao Basin, NE China. *Marine and Petroleum Geology*, *25*(4-5), 416-432.

811

Fernández-Ibáñez, F., DeGraff, J. M., & Ibrayev, F. (2018). Integrating borehole image logs with core: A method to enhance subsurface fracture characterization. AAPG Bulletin, 102(6), 1067-1090.

Ferrill, D.A., McGinnis, R.N., Morris, A.P., Smart, K.J., Sickmann, Z.T., Bents, M., Lehrmann, D and Evans, M.A. 2014. Control of mechanical stratigraphy on bed-restricted jointing and normal faulting: Eagle Ford Formation, south-central Texas. AAPG Bulletin 98, 2477–2506.

Fossen, H., Schultz, R. A., & Torabi, A. (2011). Conditions and implications for compaction band formation in the Navajo Sandstone, Utah. *Journal of Structural Geology*, *33*(10), 1477-1490.

Foster, M. E., & Hudleston, P. J. (1986). "Fracture cleavage" in the Duluth Complex, northeastern Minnesota. *Geological Society of America Bulletin*, *97*(1), 85-96.

Frost III, E. L., & Kerans, C. (2010). Controls on syndepositional fracture patterns, Devonian reef complexes, Canning Basin, Western Australia. *Journal of Structural Geology*, *32*(9), 1231-1249.

Gale, J. F., Lander, R. H., Reed, R. M., & Laubach, S. E. (2010). Modeling fracture porosity evolution in dolostone. Journal of Structural Geology, 32(9), 1201-1211.

Gale, J. F., Laubach, S. E., Olson, J. E., Eichhubl, P., & Fall, A. (2014). Natural fractures in shale: A review and new observationsNatural Fractures in Shale: A Review and New Observations. AAPG bulletin, 98(11), 2165-2216.

Gauthier, B. D. M., Auzias, V., Garcia, M., & Chiapello, E. (2002, January). Static and dynamic characterization of fracture pattern in the Upper Jurassic reservoirs of an offshore Abu Dhabi field: From well data to full field modeling. In *Abu Dhabi International Petroleum Exhibition and Conference*. Society of Petroleum Engineers.

Gillespie, P.A., Howard, C., Walsh, J.J. & Watterson, J., 1993. Measurement and characterisation of spatial distributions of fractures. Tectonophysics. 226 113-141.

Gillespie, P.A., Johnston, J.D., Loriga, M.A., McCaffrey, K.L.W., Walsh, L.L., Watterson, L., 1999. Influence of layering on vein systematics in line samples. In: McCaffrey, K.J.W., Lonergan, L., Wilkinson, J.J. (Eds.), Fractures, Fluid Flow and Mineralization. Geological Society, London, Special Publication 155, pp. 35-56.

Gillespie, P.A., Walsh, J.J., Watterson, J., Bonson, C.G. & Manzocchi, T. 2001. Scaling relationships of joints and vein arrays from The Burren, Co. Clare, Ireland. Journal of Structural Geology, 23, 183-202.

854 Gillespie, P. A., Monsen, E., Maerten, L., Hunt, D., Thurmond, J., Tuck, D. & Sullivan, M. D.
855 (2011). Fractures in carbonates: From digital outcrops to mechanical models. *Outcrops*
856 *revitalized—Tools, techniques and applications: Tulsa, Oklahoma, SEPM Concepts in*
857 *Sedimentology and Paleontology*, *10*, 137-147.

858 Graham Wall, B. R., Girbacea, R., Mesonjesi, A., & Aydin, A. (2006). Evolution of fracture and
859 fault-controlled fluid pathways in carbonates of the Albanides fold-thrust belt. AAPG
860 Bulletin, 90(8), 1227-1249.

861

862 Gross, M. R. (1993). The origin and spacing of cross joints: examples from the Monterey
863 Formation, Santa Barbara Coastline, California. *Journal of Structural Geology*, *15*(6), 737-
864 751.

865

866 Gross, M. R., Fischer, M. P., Engelder, T., & Greenfield, R. J. (1995). Factors controlling joint
867 spacing in interbedded sedimentary rocks: integrating numerical models with field
868 observations from the Monterey Formation, USA. Geological Society, London, Special
869 Publications, 92(1), 215-233.

870

871 Gross, M. R., 1998, Practical methods of fracture analysis - implications for fractured
872 reservoirs: in, Hoak, T.E., ed., Fractured Reservoirs: Practical Exploration and Development
873 Strategies, Rocky Mountain Assoc. of Geologists, p. 117-136.

874

875 Gudmundsson, A., & Løtveit, I. F. (2014). Sills as fractured hydrocarbon reservoirs: examples
876 and models. *Geological Society, London, Special Publications*, *374*(1), 251-271.

877

878 Gutmanis, J., i Oró, L. A., Díez-Canseco, D., Chebbihi, L., Awdal, A., & Cook, A. (2018).
879 Fracture analysis of outcrop analogues to support modelling of the subseismic domain in
880 carbonate reservoirs, south-central Pyrenees. Geological Society, London, Special
881 Publications, 459(1), 139-156.

882

883 Healy, D. and Blenkinsop, T. and Timms, N.E. and Meredith, P. and Mitchell, T. and Cooke,
884 M. (2015). Polymodal faulting: Time for a new angle on shear failure. Journal of Structural
885 Geology. 80: pp. 57-71.

886

887 Hestir, K., & Long, J. C. (1990). Analytical expressions for the permeability of random two-
888 dimensional Poisson fracture networks based on regular lattice percolation and equivalent
889 media theories. *Journal of Geophysical Research: Solid Earth*, *95* (B13), 21565-21581.

890

891 Hetényi, G., Taisne, B., Garel, F., Médard, É., Bosshard, S., & Mattsson, H. B. (2012). Scales of
892 columnar jointing in igneous rocks: field measurements and controlling factors. *Bulletin of*
893 *Volcanology*, *74*(2), 457-482.

894

895 Holdsworth, R.E., McCaffrey, K.J.W., Dempsey, E., Roberts, N.M.W., Hardman, K., Morton,
896 A., Feely, M., Hunt, J., Conway, A., Robertson, A. 2019. Natural fracture propping and

897   earthquake-induced oil migration in fractured basement reservoirs. Geology, 47,
898   https://doi.org/10.1130/G46280.1

899

900   Hooker, J. N., Laubach, S. E., & Marrett, R. (2013). Fracture-aperture size—Frequency,
901   spatial distribution, and growth processes in strata-bounded and non-strata-bounded
902   fractures, Cambrian Mesón Group, NW Argentina. Journal of Structural Geology, 54, 54-71.

903

904   Hooker, J.N., Laubach, S.E., and Marrett, R., 2014. A universal power-law scaling exponent
905   for fracture apertures in sandstone. Geological Society of America Bulletin 126(9-10), 1340-
906   1362. doi: 10.1130/B30945.1

907

908   Huang, Q., Angelier, L., 1989. Fracture spacing and its relation to bed thickness. Geological
909   Magazine 126, 550-556.

910

911   Hunt, D. W., Fitchen, W. M., & Kosa, E. (2003). Syndepositional deformation of the Permian
912   Capitan reef carbonate platform, Guadalupe Mountains, New Mexico, USA. *Sedimentary*
913   *Geology*, *154*(3-4), 89-126.

914

915   Johri, M., Zoback, M. D., & Hennings, P. (2014). A scaling law to characterize fault-damage
916   zones at reservoir depths. *AAPG Bulletin*, *98*(10), 2057-2079.

917

918   Kaminskaite, I., Fisher, Q. J., & Michie, E. A. H. (2019). Microstructure and petrophysical
919   properties of deformation bands in high porosity carbonates. *Journal of Structural*
920   *Geology*, *119*, 61-80.

921

922   Kim, Y. S., Peacock, D. C. P., & Sanderson, D. J. (2003). Mesoscale strike-slip faults and
923   damage zones at Marsalforn, Gozo Island, Malta. *Journal of Structural Geology*, *25*(5), 793-
924   812.

925

926   Koning, T. (2003). Oil and gas production from basement reservoirs: examples from
927   Indonesia, USA and Venezuela. *Geological Society, London, Special Publications*, *214*(1), 83-
928   92.

929

930   Laubach, S. E. (2003). Practical approaches to identifying sealed and open fractures. *AAPG*
931   *bulletin*, *87*(4), 561-579.

932

933 Laubach, S. E., Reed, R. M., Olson, J. E., Lander, R. H., & Bonnell, L. M. (2004). Coevolution of
934 crack-seal texture and fracture porosity in sedimentary rocks: cathodoluminescence
935 observations of regional fractures. Journal of Structural Geology, 26(5), 967-982.

936

937 Laubach, S. E., Olson, J. E., & Gross, M. R. (2009). Mechanical and fracture stratigraphy.
938 *AAPG bulletin*, *93* (11), 1413-1426.

939

940 Laubach, S. E., Fall, A., Copley, L. K., Marrett, R., & Wilkins, S. J. (2016). Fracture porosity creation
941 and persistence in a basement-involved Laramide fold, Upper Cretaceous Frontier Formation, Green
942 River Basin, USA. *Geological Magazine*, *153*(5-6), 887-910.

943

944 Laubach, S. E., Lamarche, J., Gauthier, B. D., Dunne, W. M., & Sanderson, D. J. (2018). Spatial
945 arrangement of faults and opening-mode fractures. Journal of Structural Geology, 108, 2-15.

946

947 Laubach, S.E., Lander, R.H., Criscenti, L.J., et al., 2019. The role of chemistry in fracture
948 pattern development and opportunities to advance interpretations of geological materials.
949 Reviews of Geophysics, 57 (3), 1065-1111. doi:10.1029/2019RG000671

950

951 Ledésert, B., Hebert, R., Genter, A., Bartier, D., Clauer, N., & Grall, C. (2010). Fractures,
952 hydrothermal alterations and permeability in the Soultz Enhanced Geothermal
953 System. Comptes Rendus Geoscience, 342(7-8), 607-615.

954

955 Li, J. Z., Laubach, S. E., Gale, J. F. W., & Marrett, R. A. (2018). Quantifying opening-mode
956 fracture spatial organization in horizontal wellbore image logs, core and outcrop: application
957 to Upper Cretaceous Frontier Formation tight gas sandstones, USA. Journal of Structural
958 Geology, 108, 137-156.

959

960 Lima, B. E. M., & De Ros, L. F. (2019). Deposition, diagenetic and hydrothermal processes in
961 the Aptian Pre-Salt lacustrine carbonate reservoirs of the northern Campos Basin, offshore
962 Brazil. *Sedimentary Geology*, *383*, 55-81.

963

964 Long, J. C., & Witherspoon, P. A. (1985). The relationship of the degree of interconnection to
965 permeability in fracture networks. Journal of Geophysical Research: Solid Earth, 90(B4),
966 3087-3098.

967

968 Loucks, R. G. (1999). Paleocave carbonate reservoirs: Origins, burial-depth modifications,
969 spatial complexity, and reservoir implications. *AAPG bulletin*, *83*(11), 1795-1834.

970

971 Lu, S. M. (2018). A global review of enhanced geothermal system (EGS). Renewable and
972 Sustainable Energy Reviews, 81, 2902-2921.

973

974 Maerten, L., Legrand, X., Castagnac, C., Lefranc, M., Joonnekindt, J. P., & Maerten, F. (2019).
975 Fault-related fracture modeling in the complex tectonic environment of the Malay basin,
976 offshore Malaysia: an integrated 4D geomechanical approach. *Marine and Petroleum*
977 *Geology*, *105*, 222-237.

978

979 Magara, K. (2003). Volcanic reservoir rocks of northwestern Honshu Island,
980 Japan. *Geological Society, London, Special Publications*, *214*(1), 69-81.

981

982 Manzocchi, T. (2002). The connectivity of two-dimensional networks of spatially correlated
983 fractures. *Water Resources Research*, *38*(9), 1-1.

984

985 Mazzullo, S. J., & Harris, P. M. (1992). Mesogenetic dissolution: its role in porosity
986 development in carbonate reservoirs. *AAPG bulletin*, *76*(5), 607-620.

987

988 Mazzullo, S. J., & Chilingarian, G. V. (1996). Hydrocarbon reservoirs in karsted carbonate
989 rocks. In Developments in Petroleum Science (Vol. 44, pp. 797-865). Elsevier.

990

991 McNamara, D. D., Massiot, C., & Milicich, S. M. (2017). Characterizing the subsurface
992 structure and stress of New Zealand's geothermal fields using borehole images. *Energy*
993 *Procedia*, *125*, 273-282.

994

995 Micarelli, L., Benedicto, A., & Wibberley, C. A. J. (2006). Structural evolution and
996 permeability of normal fault zones in highly porous carbonate rocks. *Journal of Structural*
997 *Geology*, *28*(7), 1214-1227.

998

999 Morris, A. P., Ferrill, D. A., & McGinnis, R. N. (2009). Mechanical stratigraphy and faulting in
1000 Cretaceous carbonates. *AAPG bulletin*, *93*(11), 1459-1470.

Müller, C., Siegesmund, S., & Blum, P. (2010). Evaluation of the representative elementary volume (REV) of a fractured geothermal sandstone reservoir. *Environmental earth sciences*, *61*(8), 1713-1724.

Narr, W., & Suppe, J. (1991). Joint spacing in sedimentary rocks. *Journal of Structural Geology*, *13*(9), 1037-1048.

Narr, W., & Flodin, E. (2012, April). Fractures in steep-rimmed carbonate platforms: Comparison of Tengiz Reservoir, Kazakhstan, and outcrops in Canning Basin, NW Australia. In *American Association of Petroleum Geologists, Annual Convention and Exhibition, Long Beach, California*.

Narr, W., Schechter, D. S., & Thompson, L. B. (2006). *Naturally fractured reservoir characterization* (Vol. 112). Richardson, TX: Society of Petroleum Engineers.

Nelson, R. (2001). *Geologic analysis of naturally fractured reservoirs*. Elsevier.

Nguyen, N. T. B., Dang, C. T. Q., Bae, W., Chen, Z., Nguyen, A., & Thuoc, P. H. (2011, January). Geological characteristics and integrated development plan for giant naturally fractured basement reservoirs. In *Canadian Unconventional Resources Conference*. Society of Petroleum Engineers 149510.

Nixon, C. W., Vaagan, S., Sanderson, D. J., & Gawthorpe, R. L. (2019). Spatial distribution of damage and strain within a normal fault relay at Kilve, UK. *Journal of Structural Geology*, *118*, 194-209.

Nolting, A., Zahm, C. K., Kerans, C., & Alzayer, Y. (2020). The influence of variable progradation to aggradation ratio and facies partitioning on the development of syndepositional deformation in steep-walled carbonate platforms. *Marine and Petroleum Geology*, *114*, 104171.

Nosjean, N., Khamitov, Y., Rodriguez, S., & Yahia-Cherif, R. (2020). Fracture corridor identification through 3D multifocusing to improve well deliverability, an Algerian tight reservoir case study. Solid Earth Sciences, 5(1), 31-49.

1036

1037 Odling, N. E., Gillespie, P., Bourgine, B., Castaing, C., Chiles, J. P., Christensen, N. P., ... &
1038 Trice, R. (1999). Variations in fracture system geometry and their implications for fluid flow
1039 in fractures hydrocarbon reservoirs. *Petroleum Geoscience*, *5*(4), 373-384.

1040

1041 Olson, J. E. (2004). Predicting fracture swarms—The influence of subcritical crack growth
1042 and the crack-tip process zone on joint spacing in rock. Geological Society, London, Special
1043 Publications, 231(1), 73-88.

1044

1045 Olson, J. E., Laubach, S. E., & Lander, R. H. (2009). Natural fracture characterization in tight gas
1046 sandstones: Integrating mechanics and diagenesis. *AAPG bulletin*, *93*(11), 1535-1549.

1047

1048 Ortega, O. J., Marrett, R. A., & Laubach, S. E. (2006). A scale-independent approach to fracture
1049 intensity and average spacing measurement. *AAPG bulletin*, *90*(2), 193-208.

1050

1051 Ozkaya, S. I. (2007). Detection of fracture corridors from openhole logs in horizontal wells.
1052 In SPE Saudi Arabia Section Technical Symposium. Society of Petroleum Engineers.

1053

1054 P'an, C. H. (1982). Petroleum in basement rocks. AAPG Bulletin, 66(10), 1597-1643.

1055

1056 Paul, P. K., Zoback, M. D., & Hennings, P. H. (2009). Fluid flow in a fractured reservoir using a
1057 geomechanically constrained fault-zone-damage model for reservoir simulation. SPE
1058 Reservoir Evaluation & Engineering, 12(04), 562-575.

1059

1060 Philip, Z. G., Jennings Jr, J. W., Olson, J. E., & Holder, J. (2005). Modeling coupled fracture-
1061 matrix fluid flow in geomechanically simulated fracture networks. In SPE Annual Technical
1062 Conference and Exhibition. Society of Petroleum Engineers.

1063

1064 Pearce, M. A., Jones, R. R., Smith, S. A., & McCaffrey, K. J. (2011). Quantification of fold
1065 curvature and fracturing using terrestrial laser scanning. AAPG Bulletin, 95(5), 771-794.

1066

1067 Poppelreiter, M., Garcia-Carballido, C., & Kraaijveld, M. (2010). Borehole image log
1068 technology: application across the exploration and production life cycle.

1069

1070 Price, N. J., & Cosgrove, J. W. (1990). Analysis of geological structures. Cambridge University
1071 Press.

1072

1073 Pyrak-Nolte, L. J., & Morris, J. P. (2000). Single fractures under normal stress: The relation
1074 between fracture specific stiffness and fluid flow. International Journal of Rock Mechanics
1075 and Mining Sciences, 37(1-2), 245-262.

1076

1077 Questiaux, J. M., Couples, G. D., & Ruby, N. (2010). Fractured reservoirs with fracture
1078 corridors. Geophysical Prospecting, 58(2), 279-295.

1079

1080 Rawnsley, K. D., Rives, T., Petit, J. P., Hencher, S. R., & Lumsden, A. C. (1992). Joint
1081 development in perturbed stress fields near faults. Journal of Structural Geology, 14(8-9),
1082 939-951.

1083

1084 Rotevatn, A., & Bastesen, E. (2014). Fault linkage and damage zone architecture in tight
1085 carbonate rocks in the Suez Rift (Egypt): implications for permeability structure along
1086 segmented normal faults. Geological Society, London, Special Publications, 374(1), 79-95.

1087

1088 Salah, M. G., & Alsharhan, A. S. (1998). The Precambrian basement: a major reservoir in the
1089 rifted basin, Gulf of Suez. Journal of Petroleum Science and Engineering, 19(3-4), 201-222.

1090

1091 Salomão, M. C., Marçon, D. R., Rosa, M. B., de Salles Pessoa, T. C., & Capeleiro Pinto, A. C.
1092 (2015). Broad Strategy to Face with Complex Reservoirs: Expressive Results of Production in
1093 Pre-Salt Area, Offshore Brasil. Offshore Technology Conference. doi:10.4043/25712-MS.

1094

1095 Sammis, C. G., An, L., & Ershaghi, I. (1992). Determining the 3-D fracture structure in the
1096 Geysers geothermal reservoir (No. SGP-TR-141-13). University of Southern California, Los
1097 Angeles, CA.

1098

1099 Sanderson, D. J., & Nixon, C. W. (2015). The use of topology in fracture network
1100 characterization. Journal of Structural Geology, 72, 55-66.

1101

1102 Sanderson, D. J., & Nixon, C. W. (2018). Topology, connectivity and percolation in fracture
1103 networks. Journal of Structural Geology, 115, 167-177.

1104

1105 Schill, E., Genter, A., Cuenot, N., & Kohl, T. (2017). Hydraulic performance history at the
1106 Soultz EGS reservoirs from stimulation and long-term circulation tests. Geothermics, 70,
1107 110-124.

1108

1109 Schöpfer, M. P., Arslan, A., Walsh, J. J., & Childs, C. (2011). Reconciliation of contrasting
1110 theories for fracture spacing in layered rocks. Journal of Structural Geology, 33(4), 551-565.

1111

1112 Segall, P., Pollard, D.D., 1983. Joint formation in granitic rocks of the Sierra Nevada.
1113 Geological Society of America Bulletin 94, 563-575.

1114

1115 Shackleton, J. R., Cooke, M. L., Vergés, J., & Simó, T. (2011). Temporal constraints on
1116 fracturing associated with fault-related folding at Sant Corneli anticline, Spanish
1117 Pyrenees. Journal of Structural Geology, 33(1), 5-19.

1118

1119

1120 Sharp, I., Gillespie, P., Morsalnezhad, D., Taberner, C., Karpuz, R., Vergés, J., Horbury, A.,
1121 Pickard, N., Garland, J. & Hunt, D. (2010). Stratigraphic architecture and fracture-controlled
1122 dolomitization of the Cretaceous Khami and Bangestan groups: an outcrop case study,
1123 Zagros Mountains, Iran. Geological Society, London, Special Publications, 329(1), 343-396.

1124

1125

1126 Sibson, R. H. (1996). Structural permeability of fluid-driven fault-fracture meshes. Journal of
1127 Structural Geology, 18(8), 1031-1042.

1128

1129 Smith Jr, L. B., & Davies, G. R. (2006). Structurally controlled hydrothermal alteration of
1130 carbonate reservoirs: Introduction. AAPG Bulletin, 90(11), 1635-1640.

1131

1132 Solum, J. G., & Huisman, B. A. H. (2017). Toward the creation of models to predict static and
1133 dynamic fault-seal potential in carbonates. Petroleum Geoscience, 23 (1), 70-91.

1134

1135 Spina, V., Borgomano, J., Nely, G., Shchukina, N., Irving, A., Neumann, C., & Neillo, V. (2015).
1136 Characterization of the Devonian Kharyaga carbonate platform (Russia): Integrated and
1137 multiscale approach. AAPG Bulletin, 99(9), 1771-1799.

1138

1139 Stewart, S.A. & Podolski, R. 1998. Curvature analysis of gridded geological surfaces. In:
1140 Coward, M.P., Daltaban, T.S. & Johnson, H. (eds) Structural Geology in Reservoir
1141 Characterization. Geological Society,London, Special Publications, 127, 133–147,
1142 https://doi.org/10.1144/GSL.SP.1998.127.01.11

1143

1144

1145 Strijker, G., Bertotti, G., & Luthi, S. M. (2012). Multi-scale fracture network analysis from an
1146 outcrop analogue: A case study from the Cambro-Ordovician clastic succession in Petra,
1147 Jordan. Marine and Petroleum Geology, 38(1), 104-116.

1148

1149 Tavani, S., Corradetti, A., Sabbatino, M., Morsalnejad, D., & Mazzoli, S. (2018). The Meso-
1150 Cenozoic fracture pattern of the Lurestan region, Iran: The role of rifting, convergence, and
1151 differential compaction in the development of pre-orogenic oblique fractures in the Zagros
1152 Belt. Tectonophysics, 749, 104-119.

1153

1154 Tjetland, G., Kristiansen, T. G., & Buer, K. (2007, January). Reservoir management aspects of
1155 early waterflood response after 25 years of depletion in the Valhall field. In *International*
1156 *Petroleum Technology Conference*. International Petroleum Technology Conference.
1157 doi:10.2523/IPTC-11276-MS

1158

1159 Trice, R., Hiorth, C., & Holdsworth, R. (2019). Fractured basement play development on the
1160 UK and Norwegian rifted margins. *Geological Society, London, Special Publications*, *495*,
1161 SP495-2018.

1162

1163 van Golf-Racht, T. D. (1982). *Fundamentals of fractured reservoir engineering*. Elsevier.

1164

1165 Vidal, J., & Genter, A. (2018). Overview of naturally permeable fractured reservoirs in the
1166 central and southern Upper Rhine Graben: Insights from geothermal wells. *Geothermics*, *74*,
1167 57-73.

1168

1169 Vollgger, S. A., & Cruden, A. R. (2016). Mapping folds and fractures in basement and cover
1170 rocks using UAV photogrammetry, Cape Liptrap and Cape Paterson, Victoria,
1171 Australia. *Journal of Structural Geology*, *85*, 168-187.

1172

1173 Walker, R.J., Holdsworth, R.E., Imber, J., Faulkner, D.R. & Armitage, P.J. 2013. Fault zone
1174 architecture and fluid flow in interlayered basaltic volcaniclastic crystalline sequences.
1175 Journal of Structural Geology, 51, 92-104, doi: 10.1016/j.jsg.2013.03.004

1176

1177 Wennberg, O. P., Rennan, L., & Basquet, R. (2009). Computed tomography scan imaging of
1178 natural open fractures in a porous rock; geometry and fluid flow. *Geophysical*
1179 *Prospecting*, *57*(2), 239-249.

1180

1181 Wennberg, O. P., Casini, G., Jahanpanah, A., Lapponi, F., Ineson, J., Wall, B. G., & Gillespie, P.
1182 (2013). Deformation bands in chalk, examples from the Shetland Group of the Oseberg
1183 Field, North Sea, Norway. *Journal of Structural Geology*, *56*, 103-117.

1184

1185 Wennberg, O. P., Casini, G., Jonoud, S., & Peacock, D. C. (2016). The characteristics of open
1186 fractures in carbonate reservoirs and their impact on fluid flow: a discussion. Petroleum
1187 Geoscience 22, 91-104.

1188

1189 White, W. B. (2016). Science of caves and karst: A half century of progress. *Geological*
1190 *Society of America Special Papers*, *516*, 19-33.

1191

1192 Witte, J., Bonora, M., Carbone, C., & Oncken, O. (2012). Fracture evolution in oil-producing
1193 sills of the Rio Grande Valley, northern Neuquén Basin, Argentina. AAPG bulletin, 96(7),
1194 1253-1277.

1195

1196 Woodcock, N. H., Dickson, J. A. D., & Tarasewicz, J. P. T. (2007). Transient permeability and
1197 reseal hardening in fault zones: evidence from dilation breccia textures. Geological Society,
1198 London, Special Publications, 270(1), 43-53.

1199

1200 Wu, X., Liang, L., Shi, Y., & Fomel, S. (2019). FaultSeg3D: Using synthetic data sets to train an
1201 end-to-end convolutional neural network for 3D seismic fault
1202 segmentation. *Geophysics*, *84*(3), IM35-IM45.

1203

1204 Yielding, G., Needham, T., & Jones, H. (1996). Sampling of fault populations using sub-
1205 surface data: a review. *Journal of Structural Geology*, *18*(2-3), 135-146.

1206

1207 Younes, A. I., Engelder, T., & Bosworth, W. (1998). Fracture distribution in faulted basement
1208 blocks: Gulf of Suez, Egypt. *Geological Society, London, Special Publications*, *127*(1), 167-190.

1209

1210 Zahm, C. K., & Hennings, P. H. (2009). Complex fracture development related to
1211 stratigraphic architecture: Challenges for structural deformation prediction, Tensleep
1212 Sandstone at the Alcova anticline, Wyoming. *AAPG bulletin*, *93*(11), 1427-1446.

1213

Figures

Figure 1. Summary of global frequency of fractured reservoirs according to lithology and tectonic setting at the time of trap formation. From C&C Reservoirs (2020).

Figure 2. End member fracture systems showing an organized and well-connected system of stratabound joints and non-stratabound fractures that are strongly clustered.

Figure 3. a) Stratabound joints developed limestones within a limestone/marl sequence from the Lias (Early Jurassic) at Lavernock Point, Wales. Joints are more narrowly spaced in the thinner units than in the lower, composite unit. The fracture aperture has been greatly enlarged by recent dissolution to form karst fissures. Ruler extended to 1 m. b) Clustered non-stratabound joints developed in Silurian granodiorite from Rolfsnes, western Norway. Cliff height ca 4 m.

Figure 4. Example of a conceptual model of fracturing in an extensional setting showing faults and joints and their relationship to stratigraphy (after Gross and Eyal 2007).

Figure 5. Normal fault in Cretaceous platform limestone from Maiella, Italy. The fault has a displacement of about 50 m. The brecciated fault core occurs within a lozenge and the surrounding rock is fractured, forming a damage zone. Alun Williams for scale.
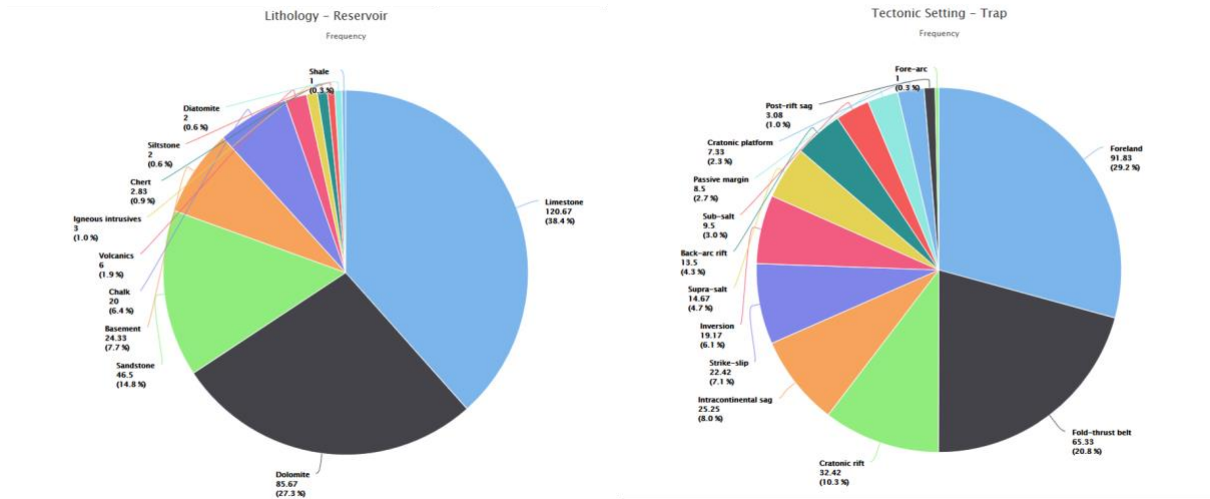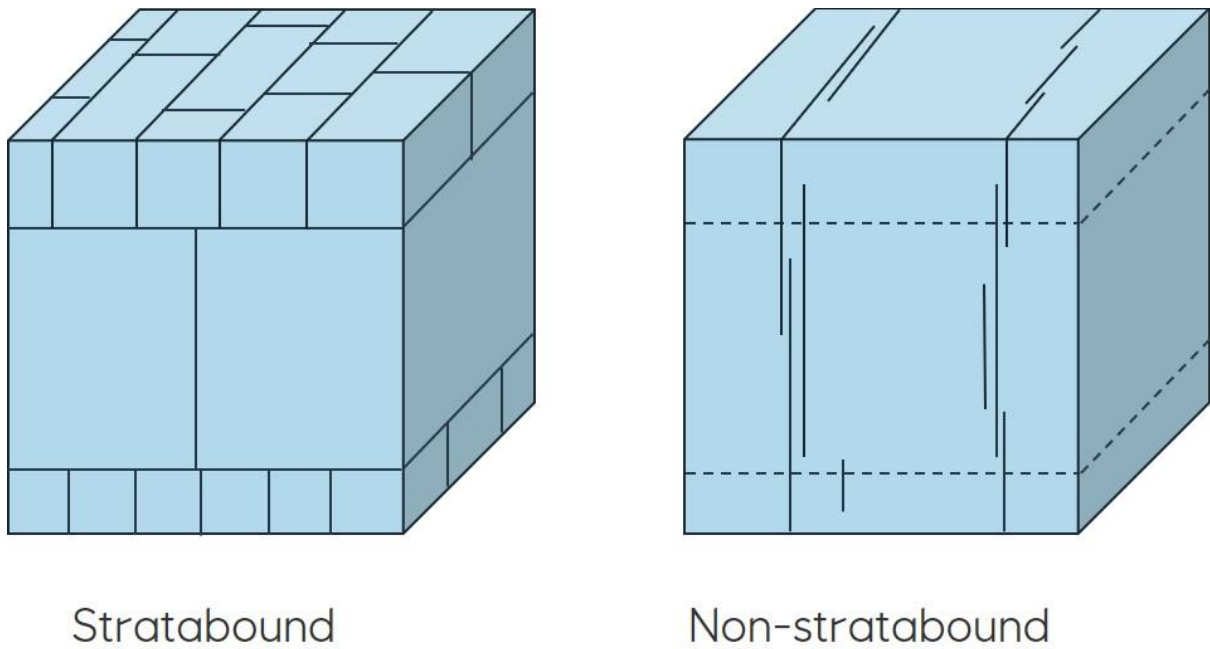
Figure 1

Figure 2

1256

1257

1258   Figure 3a and b
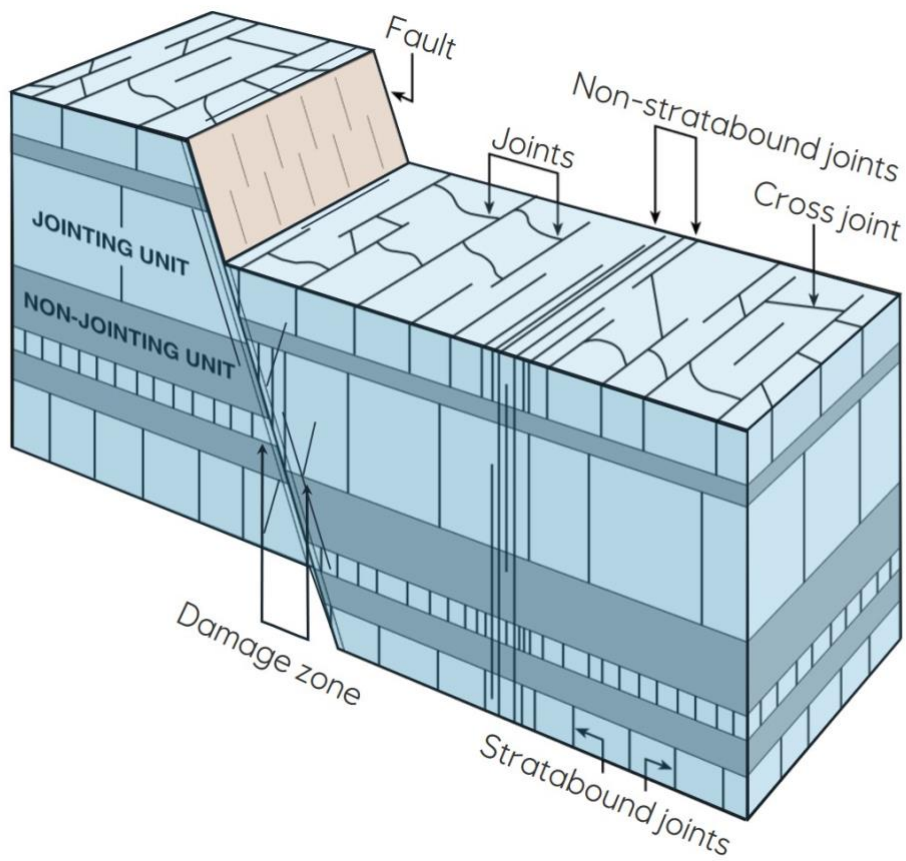
1259
1260   Figure 4

1261

1262   Figure 5

1263